Towards Acoustic Monitoring of Marine Mammals at a Tidal Turbine Site: Grand Passage, NS, Canada

Chloe E. Malinka*[#1], Alex E. Hay[*2], Richard A. Cheel[*3]

[*]*Dept. of Oceanography, Dalhousie University, Halifax, Nova Scotia, Canada*

[1]chloe.e.malinka@gmail.com, [2]alex.hay@dal.ca, [3]richard.cheel@dal.ca

[#]Now at*: Sea Mammal Research Unit, Scottish Oceans Institute, University of St Andrews, St Andrews, U.K.*

***Abstract* – There is a growing interest in extracting energy from tidal flows using in-stream kinetic energy conversion devices, and among the many questions are the possible effects on marine mammals. Underwater sound is used as a tool for detecting marine mammal presence via their vocalisations, but such Passive Acoustic Monitoring (PAM) requires an understanding of site-specific acoustic detection ranges, and the naturally occurring ambient noise in high-flow environments imposes constraints on detectability. A pilot experiment was carried out at a proposed small-scale (<2 MW) tidal energy site (Grand Passage, Nova Scotia, Canada) to partially assess the feasibility of a local PAM system. One goal was to determine the effective detection range as a function of tidal phase using sounds from a drifting underwater sound projector and moored hydrophones. A co-located acoustic Doppler flowmeter registered the near-bed water velocity. The maximum observed detection range was 700 m, with a false alarm rate of 50%. A second goal was to try different arrangements for passively reducing the effects of flow noise on the hydrophone signal. Ambient noise levels were computed for 4 different frequency bands: 0-2 kHz; 2-20 kHz; 20-50 kHz, and 50-200 kHz. On 0.5 to 1 h time scales, the bottom pod data in the 0-2 kHz band exhibited the highest variability, associated mainly with ferry and other boat traffic, and the 50-200 kHz band the least. At tidal frequencies, the clearest dependence of noise level on flow speed was in the bare hydrophone data, with the strongest dependence in the highest band, from about 48 dB re 1 µPa at slack water to about 67 dB re 1 µPa at peak tidal flow. At frequencies above 2 kHz, the data from a drifting hydrophone exhibited a pronounced dependence on position along the channel axis, comparable in magnitude to the tidal variation registered by the moored hydrophone.**

Keywords – Underwater acoustics · Passive Acoustic Monitoring · tidal energy · environmental impact · marine mammal monitoring · ambient noise · pseudosound

I. Introduction

In Nova Scotia and worldwide, high tidal flow environments are the focus of a growing effort to explore the feasibility of energy extraction using in-stream kinetic conversion devices (turbines). The Bay of Fundy experiences one of the highest tidal ranges in the world, and Fundy Tidal Inc. has proposed several small-scale (<2 MW) in-stream tidal energy projects along the Digby Neck of Nova Scotia, eastern Canada: in Grand Passage, Petit Passage and Digby Gut, with turbine deployments planned for 2015/16.

A. Monitoring Effects on Marine Mammals

Though marine renewables are generally viewed as environmentally benign, the impacts on the surrounding environment need to be comprehensively examined [1]. Among the many questions is the effect these turbines will have on marine mammals. With its temperate and nutrient-rich waters, the outer Bay of Fundy is an important feeding ground for many marine mammal species [2]. A diversity of baleen whales (mysticetes), toothed whales (odontocetes), and seals (pinnipeds) seasonally inhabit this area. These include: North Atlantic right whales, humpback whales, minke whales, fin whales, harbour porpoises, Atlantic white-sided dolphins, long-finned pilot whales, and harbour and grey seals, and other less commonly observed species [3, 4].

The marine renewable energy industry is still in its early stages, and because of this, not all of its impacts are understood, let alone assessed [5, 6]. Potential concerns for marine mammals include collision, behavioural modifications, habitat loss due to physical presence of the turbines, habitat loss due to anthropogenic noise disturbance, as well as indirect impacts due to alterations in prey populations [7, 8].

The unknown environmental effects of in-stream devices and the diversity of marine mammals in the outer Bay of Fundy suggest the tidal project's environmental impact assessment should include Passive Acoustic Monitoring (PAM) of noises, including: marine mammal sounds, natural environmental noise, and turbine-generated noise. Using underwater sound as a tool for detecting marine mammal presence via their vocalisations seems an obvious choice. Additionally, it is essential that baseline acoustic conditions be determined prior to turbine installation in order to evaluate potential disturbance impacts associated with marine energy devices [9].

B. Challenges to Acoustic Monitoring in a High Flow Environment

PAM for marine mammals at tidal energy sites requires an understanding of the site-specific acoustics affecting acoustic detection ranges. Acoustic detection thresholds for marine mammal vocalisations will vary with background noise levels, which are a function of tidal flow speed: the faster the tidal flow, the louder the ambient noise level, the smaller the acoustic detection range [3, 9].

Flow-induced self-noise (pseudosound) is also an issue. This non-propagating sound is created by turbulent pressure fluctuations in the hydrophone boundary layer and by strong currents flowing past the hydrophone [10]. A stationary hydrophone in a high-flow environment will sense these non-acoustic pressure variations, just as it senses propagating

sound pressures [10, 11]. Pseudosound is apparent only to the receiver, and can account for high noise levels at lower frequencies (<1 kHz) [12]. If sufficiently intense, pseudosound can mask sounds of interest [10]. The effective acoustic detection range of a vocalising marine mammal at a tidal energy site could be increased if this pseudosound is reduced. This idea has previously been explored [13, 15], whereby hydrophones screened tightly with polyurethane foam have been shown to act as an acoustic shield to minimize flow noise by reducing the effects of drag at modest flow speeds of ~0.5 m/s.

C. *Study Objectives*

This study investigates the acoustics of Grand Passage in relation to a future PAM system for marine mammals. The objectives of this study are:

1) To determine how noisy Grand Passage is prior to turbine installation, and to determine how sound pressure levels change with tidal flow;

2) To partially assess the feasibility of a PAM system for marine mammals in Grand Passage, by estimating acoustic detection ranges of projected sounds in part of the frequency range occupied by marine mammal vocalisations; and

3) To test if pseudosound on the hydrophone can be reduced with open-cell foam shielding.

II. Methods

A. *Study Site and Experimental Methodology*

Grand Passage is located on the eastern side of the Bay of Fundy. It is oriented north-south between Brier Island and Long Island, along the Digby Neck of Nova Scotia, Canada, connecting St. Mary's Bay to the Bay of Fundy. Grand Passage is subject to semi-diurnal tides, has a 6 m tidal range, and has surface tidal flows in excess of 4.3 m/s, with a flood tide running from south to north [15, 16]. The passage is 0.75 km wide at its widest point, and is 4.25 km long, measured from the northern tip of Brier Island to the southern tip of Long Island (Fig. 1). The bottom type is very heterogeneous, ranging from bedrock outcrops to mobile sediments consisting of a mixture of gravel, fine sand and shell hash [17]. A diesel engine ferry typically makes at least two crossings per hour during the day, and runs on demand at night.

Fieldwork was conducted from July 5-9 2012, and focused on the northern end of Grand Passage (Fig. 1). Instrumentation was deployed and recovered with a fishing vessel, the *Expectations XL* (Westport, NS). A rigid-hull inflatable boat (RHIB) was used for all other aspects of the experiment. All field tests were conducted during a spring tide to obtain conservative estimates of acoustic detection ranges.

1) *Instrumentation*: An Ocean Sonics hydrophone (*ic*Listen High Frequency) continuously collected ambient noise time series data in both FFT (Fast Fourier Transform) and WAV file format (Table 1). The response of the *ic*Listen is flat (+/- 3 dBV) over 0.01-200 kHz. The manufacturer-supplied calibration for the hydrophone was used to convert voltage to sound pressure level.

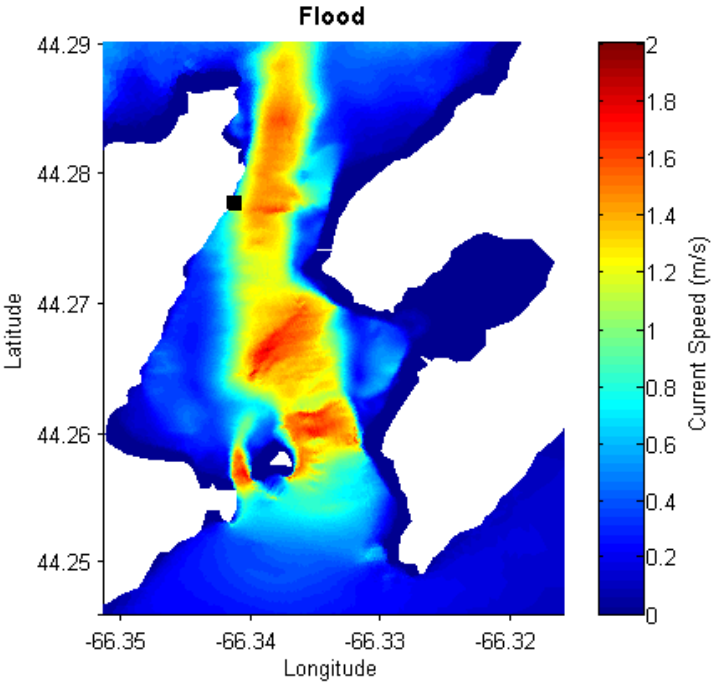

Fig. 1 Mean current speed during flood tide in Grand Passage. Current speed data are a synthesis of ADCP measurements, multi-beam WASSP® bathymetry, and a 2-dimensional numerical simulation for tidal currents. The mean moored hydrophone location is represented by a black square. (Courtesy of J. McMillan).

TABLE I
HYDROPHONE SETTINGS USED.

Parameter	FFT	WAV
Bandwidth (kHz)	204.8	102.4
Sample rate (kSamples/s)	512	256
Spectrum update rate	0.25	-
Processing mode	Mean	-
Spectrum length (points)	1024	-
Spectra per averaging interval	125	-
Resolution (Hz)	500	-

The autonomous hydrophone was moored on a fiberglass platform ballasted by three 50 lb lead weights (Fig. 2). This bottom pod set-up varied in order to investigate pseudosound reduction techniques. All cables on the platform were secured with zip ties to eliminate flapping noise.

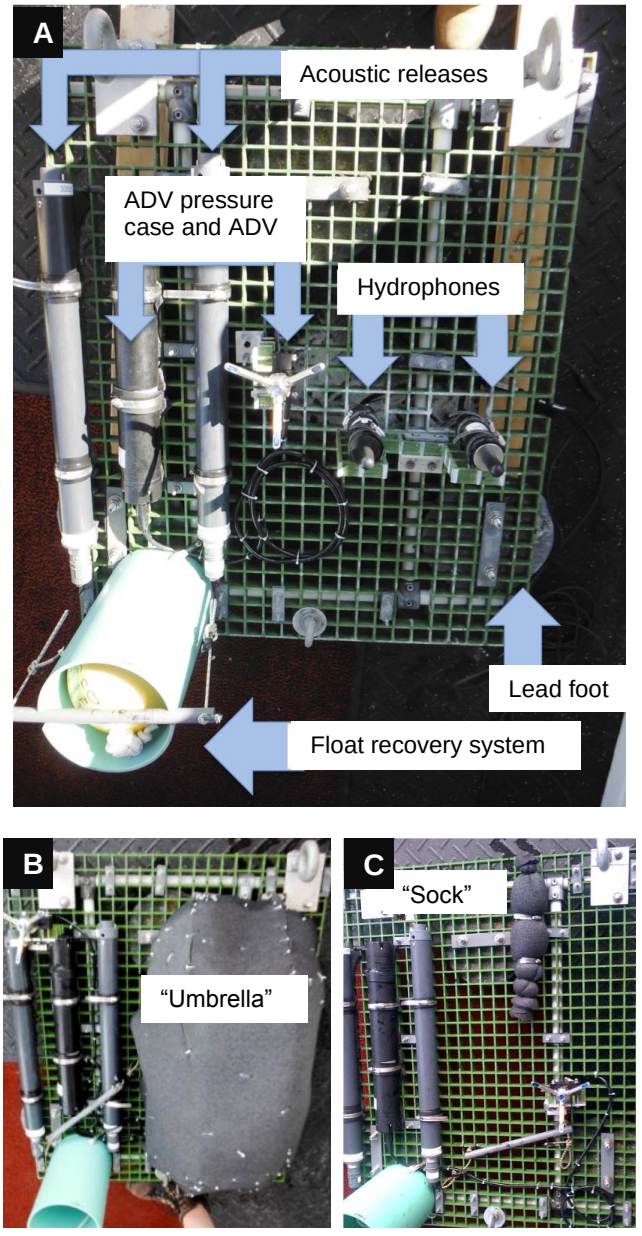

Fig. 2 Sample photos of bottom pods, showing: A) the vertical hydrophone set-up, B) the "umbrella" set-up, and C) the "sock" set-up.

An Ocean Sonics underwater projector (*ic*Talk MF Smart Projector) was used to broadcast sounds from the RHIB while drifting (engine off). Omnidirectional sounds transmitted in consecutive 5 second chirps at known times, at the maximum sound pressure level of the instrument, and spanning the instrument's full bandwidth (2-20 kHz at 101 dB re 1 µPa @ 1 m). This frequency range overlaps with the vocal ranges of some marine mammal species, and a chirp was used to test detections. The duration of each frequency (kHz) in the chirp was ~0.3 ms. Chirps were created in Audacity (<http://audacity.sourceforge.net/>). The projector was suspended from the RHIB at ~2 m below the water surface.

The RHIB position during the sound projection drifts was recorded using on-board GPS. Drifts started ~800 m upstream of the moored hydrophone, and continued until about the same distance downstream, and were carried out during flood, high slack, and ebb tides. The number of drifts completed in a day (maximum of 16) was limited by the battery life of the autonomous hydrophone (~8 h).

A Nortek Vector acoustic Doppler velocimeter (ADV) mounted on the bottom pod (Fig. 2) continuously sampled the flow velocity. The ADV sample rate and velocity range had to be adjusted after the first deployment due to data quality issues associated with the low scatterer concentrations in the water, despite being close to the seabed. On 5 July 2012, the ADV was positioned on its side, and on 6-8 July 2012 the ADV was positioned vertically, resulting in two different sample heights (0.19 m and 0.35 m) above the seabed.

On 5-7 July 2012 a second hydrophone was suspended below the RHIB at ~1.5 m below the water surface, simultaneous with sound projection drifts. Since this hydrophone was drifting with the current, pseudosound contamination was anticipated to be reduced compared to the moored hydrophone. Sound projection drifts were repeated over four days to accommodate variations in bottom pod configuration.

2) *Bottom pod deployments*: The hydrophone frame was deployed during the first low slack water of the day. The frame was deployed at nominally the same location in the northwest of Grand Passage for each of the four tests (at ~44.2776°N, 66.3412°W). A shallow location (12.8 m to 16.5 m at low water) was chosen to allow for pod recovery by SCUBA divers, if necessary. Sound projections occurred through flood and ebb tides, and at the second daily slack water (~12 h later), the frame was retrieved. A Sub Sea Sonics acoustic interrogator (model ARI-60) transmitted commands to trigger the release of the float recovery system.

Four frame set-ups designed to test pseudosound reduction techniques were used. On 5 July 2012, the hydrophone was bare and horizontal. On 6 July 2012, the hydrophone was horizontal and wrapped in open-cell, 10 pores per inch (ppi) polyurethane foam (2 cm thick overall) to make up a "sock" set-up (Fig. 2c). On 7 July 2012, the hydrophone was vertical underneath a foam shell (Fig. 2b). A dome-shaped metal frame, or "umbrella", was covered with two layers of foam (2 cm thick overall) and reinforced with galvanized wire screening. A metal cage surrounded the hydrophone sensor to prevent direct contact with the foam for both the "sock" and "umbrella" set-ups. On 8 July 2012, the sensor was bare and vertically oriented (Fig. 2a). Prior to deployment each day, detergent was applied to the hydrophone sensor to reduce surface tension, and in set-ups where foam was used, the foam was saturated with soapy water prior to deployment.

3) *Ambient Noise Drifter Trajectories*: A drifting hydrophone set-up was employed to reduce the flow noise by recording in conditions with no anticipated pseudosound. The drifter consisted of a hydrophone attached to a surface buoy by a bungee cord, suspended at ~4 m below the water surface (Fig. 3). The hydrophone was configured as before (Table 1).

Two chimney sweep brushes acted as dampers to decouple the hydrophone from the movement of the surface float. An attached global positioning system (Garmin GPS) tracked position at a sample rate of 1 Hz. The drifter (Fig. 3) was repeatedly released on 9 July 2012 in ~25 m water depth along the northwest side of Grand Passage. To account for variations in background noise level with tidal state, two drifts occurred during flood tide (sea state 2), and two drifts during high slack water (sea state 3). Boat traffic presence and sea state were recorded from visual observation over this time period.

Fig. 3 Ambient noise drifter.

4) *Ancillary Measurements*: Wind speed and direction were measured hourly at the Coast Guard station at the north end of the passage. Wind speed was also estimated during the drifts using the Beaufort wind scale. Boat traffic presence in the vicinity of the moored hydrophone was recorded from visual observations during sound projection and free-drift experiments.

The water column in Grand Passage was repeatedly profiled at various locations in the passage over four days using an RBR CTD (Conductivity Temperature Depth sensor, model XR-620CTDmF).

B. *Data Analysis*

All data analysis was done using custom scripts in Matlab (The Mathworks Inc.).

1) GPS Data: The start and end times from the RHIB tracks for each drift were used to identify and join consecutive hydrophone FFT files corresponding to each drift. Ambient noise drifter speed was determined from the GPS tracks and then time-aligned with acoustic data from the drifter by interpolating the GPS time base onto the hydrophone time base.

2) ADV Data: Velocity data were averaged over 5 minute intervals, and current speed was determined. It was discovered that the particular ADV used had a firmware error, since corrected by the manufacturer, which resulted in unusable compass readings, and therefore the orientation of the frame on the seafloor could not be reliably determined from instrument heading. The sign of the *x,y,z* velocities, together with outputs from both Acoustic Doppler Current Profiler (ADCPs) measurements from Grand Passage and a 2D numerical tidal current model in the passage [16], were used to determine the frame's orientation relative to the flow. At the hydrophone frame location, the angles of flood and ebb tide are 11.5° and 193° clockwise from true North, respectively [16].

3) Acoustic Data: Four frequency bands were selected for ambient noise level analysis: low (0-2 kHz), mid-low (2-20 kHz), mid-high (20-50 kHz), and high (50-200 kHz). These bands were selected based on a combination of biological and practical reasons. For example, pseudonoise and ferry noise is mainly <2 kHz, the chirp was from 2-20 kHz, and sediment-generated noise extends to higher frequencies. Additionally, marine mammals are often grouped by the frequencies of their vocalisations. For example, large mysticetes whales vocalise at low frequencies (several tens of Hz to several kHz), and the whistles and echolocation clicks of odontocetes range from a few hundreds of Hz to over one hundred kHz. Data in each of the four frequency bands were averaged over 10 s intervals (5,000 spectra per interval). Spectra were computed using a Hanning window with 50% overlap. Spectra computed from WAV files and those of the corresponding FFT files, computed by the instrument itself, agreed with one another.

Time series of noise levels (dB re 1 μPa) were analysed for each frequency band, for all four bottom pod deployments and the ambient noise drifts. Analyses of noise level as a function of current speed for the bottom pod, and of noise level as a function of drifter speed for the drifter, were completed. Fig. 4 shows *ic*Talk-projected sounds in the hydrophone record, and illustrates the variability in low-frequency background noise levels.

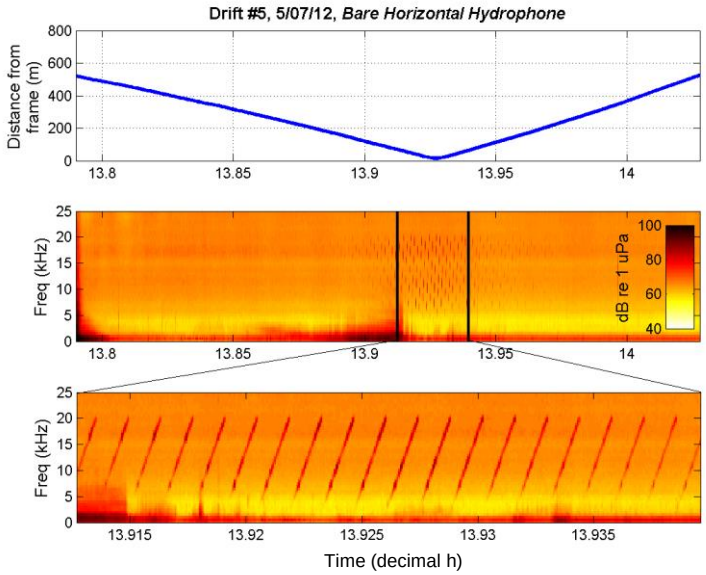

Fig. 4 A) Data segment corresponding to one RHIB drift, showing the distance from the bottom pod of the drifting RHIB projecting sounds; B) A spectrogram from the *ic*Listen on the bottom pod; and C) Zoom showing signal from *ic*Talk (2-20 kHz).

An analysis of sound detection versus range from the hydrophone was completed. A chirp correlator algorithm was constructed to detect the projected sounds in the data records registered by the hydrophone on the bottom pod, as illustrated in Fig. 5. The correlator operates in the time-frequency domain of the spectrogram. The algorithm is based on the lagged cross-correlation between a synthetic chirp spectrogram and the observed spectrogram. The synthetic chirp, $C(f,t)$, is a linear frequency sweep of unit amplitude between 2 and 20 kHz. The output of the correlator, Corr(τ), is the sum over frequency of the convolution in time of the product of the synthetic chirp and the observed spectrum, $S(f,t)$: *i.e.*

$$\mathrm{Corr}(\tau) = \sum\sum S(f_i, t_j)\, C(f_i, t_j + \tau)$$

where the double summation is over the indices i and j. The normalized correlations were sometimes contaminated by the low frequency sound evident in Fig. 5a, usually due to boat traffic and resulted in low frequency variability in the background correlation level. An example of the output of the chirp correlator is shown in Fig. 5b. The difference in correlation (ΔCorr) effectively removed this low frequency variability for all hydrophone records (Fig. 5c), and ΔCorr was used in further analysis.

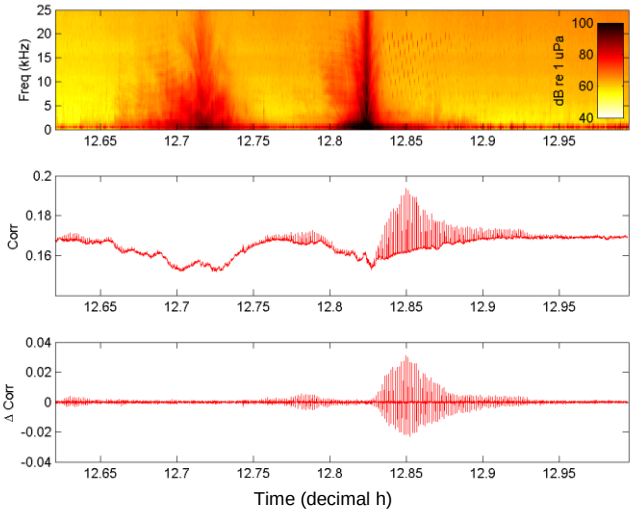

Fig. 5 Peak detection for a sample drift. A) Spectrogram from bottom pod hydrophone, where loud spikes show boat noise; B) Normalized correlation of projected sound to received sound; and C) Difference in correlation of projected sound to received sound.

A peak detection algorithm identified maxima and minima in ΔCorr values in each 5 s interval corresponding to the duration of the projected chirp (Fig. 6). To identify false alarms, the highest peak in ΔCorr value was used as a central reference. Using the 5 s chirp repetition interval, detections were considered to be a false alarm if they did not occur at multiples of 5 + 0.3 s from this reference point (Fig. 6). Data points of ΔCorr were positioned 0.25 s apart, so a + 0.3 s deviation allowed for a wavering of one data point. Only true detections were used in further analysis.

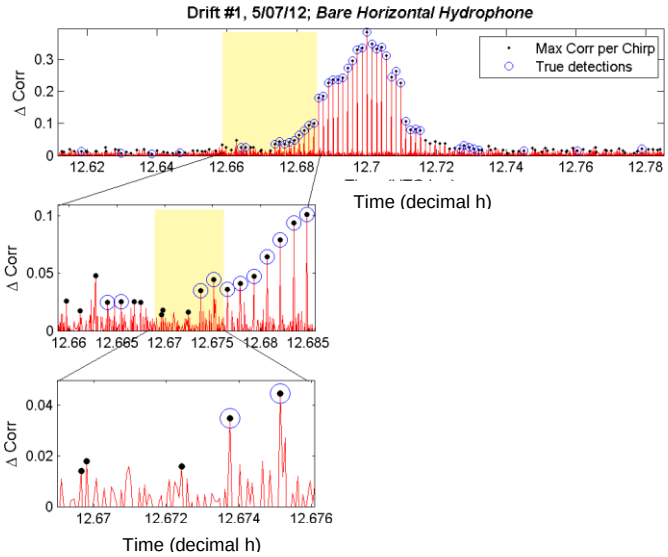

Fig. 6 Difference in correlation of projected sound to sound received by hydrophone for a sample drift. Shaded regions show the area zoomed in below. Black points show the maximum correlation per 5 s interval. Black points with blue circles show detections that lie in the 5 ± 0.3 s chirp repetition interval, and represent true detections. Black points without blue circles show false alarms.

The boat positions at the times of true detections were extracted to obtain the distances between the RHIB the bottom pod. An analysis of sound detection versus both range (m) and tidal speed (m/s) was completed to determine how acoustic detection ranges varied with tidal phase. Additionally, analyses of false alarm rate versus distance, and range at 50% false alarm rate versus current speed, were completed for each bottom pod set-up.

III. Results

A. *Water profile*

At slack water and in both flood and ebb tides, CTD measurements revealed Grand Passage to have a very well-mixed water column with no obvious stratifications. Here, the implication is that we can assume that sound speed was relatively constant.

B. *Bottom-mounted hydrophones*

1) Ambient Noise Levels: The tidal variation of the recorded ambient noise level was apparent across all bottom pod deployments. The result from the bare and vertical hydrophone deployment is shown in Figure 7. Noise levels were ~25 dB louder at peak flood compared to slack water in all four specified frequency bands.

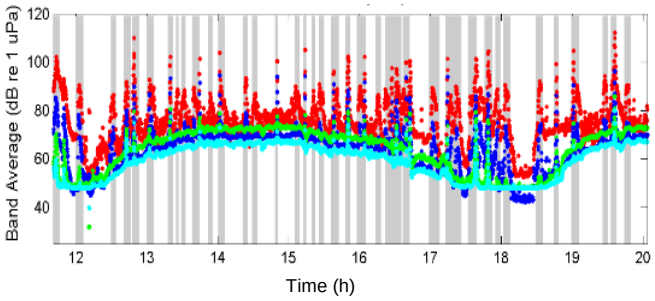

Fig. 7 Ambient noise levels detected by a hydrophone on the bottom pod (here, the bare vertical hydrophone data is shown). Shaded regions indicate field-identified noise events (*e.g.* boat passing over hydrophone or ferry crossing). Frequency bands are colour-coded, where red is 0-2 kHz, blue is 2-20 kHz, green is 20-50 kHz, and cyan is 50-200 kHz. The deployment (at ~12:00 UTC) was at low slack, and flood tide followed from 12-18 h, with peak flood at ~15:00 and high slack at ~18:00.

Mean noise levels for peak flood and peak slack water, for each deployment configuration, are presented in Table 2. The bare horizontal hydrophone, "umbrella" hydrophone, and bare vertical hydrophone records exhibited comparable noise levels across all frequency bands. Obvious high noise events (*e.g.* ferry crossings) were excluded from the values in Table 2. For these three configurations, the variation in average noise level for each of the four predefined frequency bands, across each deployment duration was small: 5 dB in the low frequency band, 6 dB in the mid-low frequency band, 3 dB in the mid-high frequency band, and 3 dB in the high frequency band.

Acoustic measurements from the "sock" hydrophone exhibited the lowest noise levels in each frequency band, of all of the bottom pod set-ups (Table 2). Compared to the mean values of noise levels of all three other bottom pod set-ups, the "sock" recorded ambient noise levels at 21, 25, 12, and 9 dB lower in the low, mid-low, mid-high, and high frequency bands, respectively, at peak flood, and recorded noise levels at 4, 5, 9, and 5 lower in the low, mid-low, mid-high, and high frequency bands, respectively, at peak slack.

TABLE II
NOISE LEVELS AT PEAK FLOOD AND SLACK WATER, FOR ALL FOUR HYDROPHONE CONFIGURATIONS ON THE BOTTOM POD.

Bottom pod set-up	**Tidal state**	**Mean noise level (dB re 1 µPa) in each frequency band (kHz)**			
		0-2	2-20	20-50	50-200
Bare vertical	Flood	78	70	73	67
	Slack	54	44	49	48
Bare horizontal	Flood	73	72	70	64
	Slack	52	43	40	36
Umbrella	Flood	72	67	71	63
	Slack	58	50	41	37
Sock	Flood	53	45	59	56
	Slack	51	41	34	35

2) *Bottom Pod Noise Level vs. Speed*: Noise levels increased as a function of current speed in all bottom pod set-ups, and only increased at current speeds >0.4 m/s for the "umbrella" set-up (Fig. 8). For each set-up, noise levels in the lowest frequency band (<2 kHz) are consistently higher. Noise levels recorded by the "sock" hydrophone were the lowest across all frequency bands, among the four bottom pod deployments. Across all comparable current speeds for the bare hydrophone set-ups (<0.6 m/s), noise levels are greater when the hydrophone is horizontal than when it is vertical, across all frequency bands. Note that the range of current speeds is smaller for the bare horizontal hydrophone because the ADV sampled closer to the seabed that day.

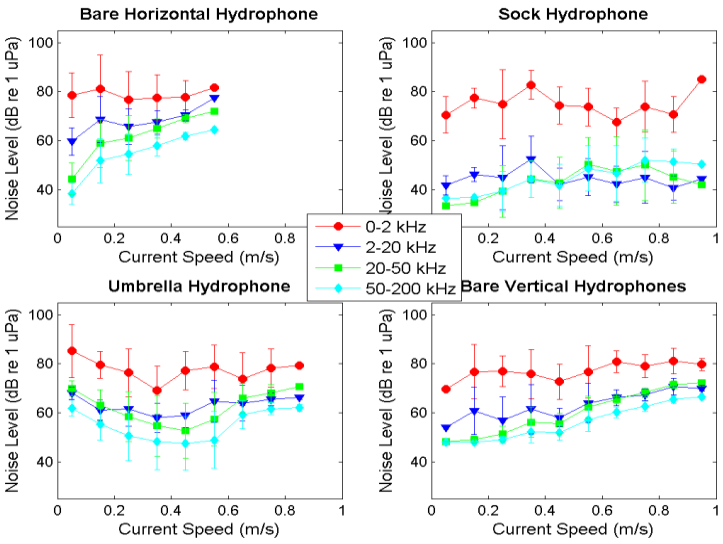

Fig. 8 Analysis of noise level as detected by the moored hydrophone as a function of current speed, for each bottom pod set-up. Current speed range is lower for the bare horizontal hydrophone because the ADV sampled closer to the seabed here.

C. *Drifter Measurements of Ambient Noise*

Four releases of the free-drifting hydrophone were performed: two during full flood, and two at high slack. Flood tide drifts lasted <30 min, and slack water drifts lasted <15 min. The peak current speed during the flood tide drifts – based on the GPS track – was 2.5 m/s, several times greater than the 1 m/s measured by the ADV on the bottom pods due to the effect of bottom friction on the velocity profile. The wind picked up during the drifts that occurred at high slack, resulting in increased noise levels in the 0-2 kHz band compared to peak flood. Otherwise, slack water noise levels were 4, 13 and 9 dB lower than during peak flood, for the mid-low, mid-high, and high frequency bands, respectively.

The noise levels registered in the higher frequency bands during the flood tide drifts exhibited a maximum as the drifter passed the location of the bottom pod deployments (Fig. 9, 10). Noise from the engines of the fishing and whale watch boats in the area extends up to 50 kHz (Fig. 9). Drifter speed was also noticeably higher midway through the drift, indicating that flow speeds are higher at this location during flood, due the narrowing of the channel in this area, and this is consistent with numerical circulation model results (Fig. 1 and [16]).

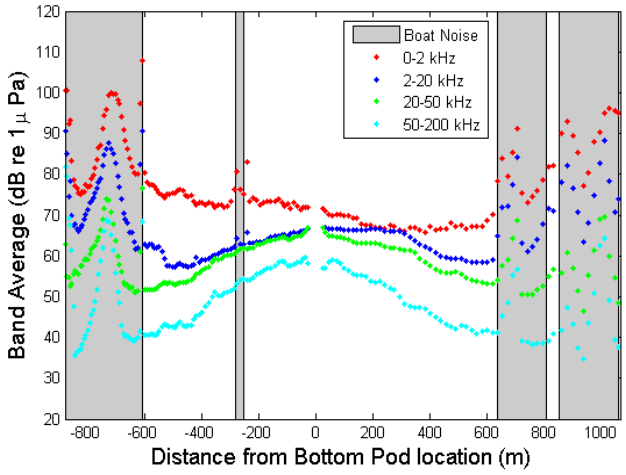

Fig. 9 Ambient noise measurements as detected by the drifting hydrophone during peak flood tide, as a function of distance from the bottom pod location. Negative distances are south of the bottom pod. Shaded regions indicate boat noise events. The total drift duration is 26 minutes.

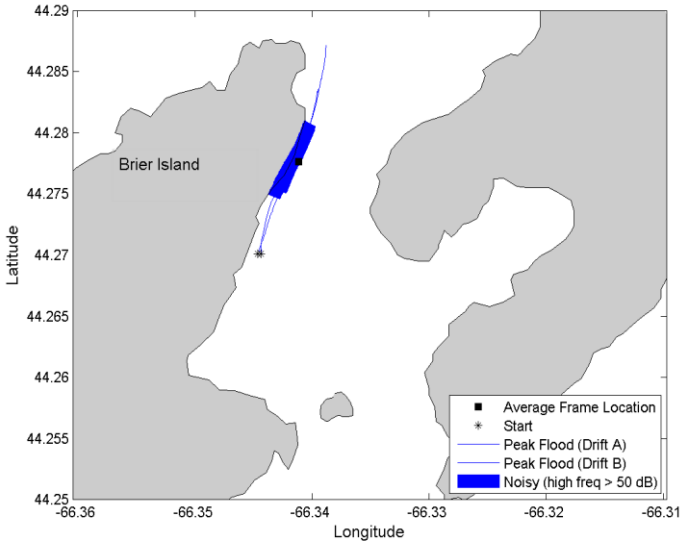

Fig. 10 Track locations of increased noise level collected by the ambient noise drifter. Noisy points were identified as when noise levels in the high frequency band (50-200 kHz) exceeded 50 dB re 1 μPa.

D. *Acoustic Detection Ranges*

Maximum ΔCorr values are greatest for the bare vertical hydrophone (Fig. 11), followed by the "sock" hydrophone. The "sock" exhibited a greatly reduced noise level in the frequency band of 2-20 kHz which aligned with sound projections. Maximum values of ΔCorr for the "sock" are not larger than other bottom pod set-ups. Maximum values of ΔCorr decreased as a function of distance from the hydrophone, for all bottom pod set-ups, except for the "umbrella". The highest ΔCorr values for the "umbrella" set-up were not as high as for the other bottom pod set-ups. It is difficult to confidently say that the "umbrella" effectively detected sound projections at a distance, since its maximum values of ΔCorr were not high at close range.

Maximum ΔCorr values were only higher when the tidal current is weaker for the bare vertical and "sock" hydrophones. For the "umbrella", this observation holds true except for when tidal current speed is low (<0.65 m/s). Maximum ΔCorr values varied less as a function of current speed for the bare horizontal hydrophone. Maximum values of ΔCorr did not exceed 0.1 at a distance of ~150 m for the bare horizontal hydrophone, ~75 m for the "sock", ~200 m for the "umbrella", and ~250 m for the bare vertical hydrophone. Acoustic detection ranges, as measured by maximum ΔCorr values, were greatest for the bare vertical hydrophone.

Maximum detection range, defined as the range at which the false alarm rate was 50%, are shown for each configuration (Fig. 12). Acoustic detection ranges were greatest for the bare vertical hydrophone, extending up to ~700 m from the bottom pod location. False alarm rates increased as a function of distance from the hydrophone for all bottom pod set-ups. Similarly, maximum detection range tended to decrease with increasing flow speed for all four set-ups.

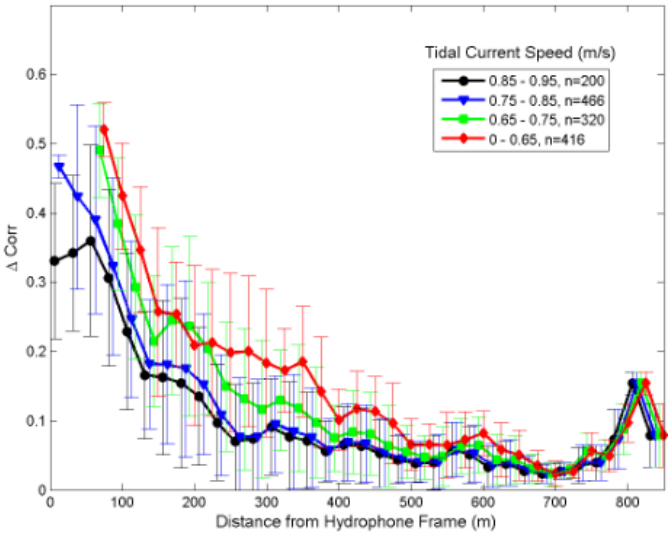

Fig. 11 Acoustic detection ranges and false alarm rate for the bare horizontal hydrophone, showing the difference in peak correlation of the projected and received sounds, as a function of distance from the hydrophone. Current speeds are colour-coded to show acoustic detection range as a function of tidal phase.

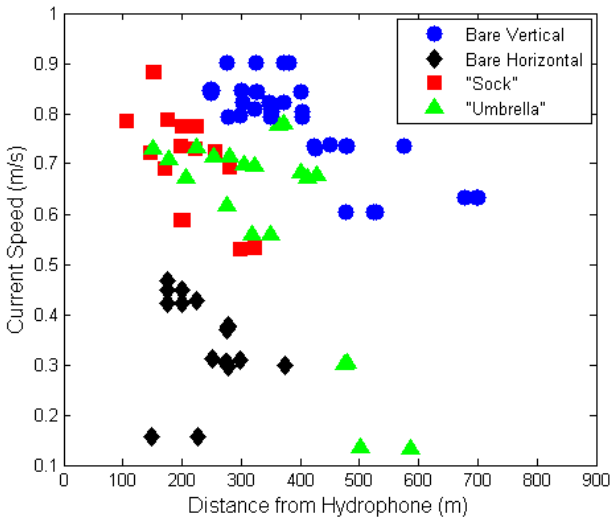

Fig. 12 Maximum chirp detection range – the ranges at which the false alarm rate was 50%. Note the increase in maximum detection with decreasing current speed for the bare vertical hydrophone.

IV. Discussion

A. *Ambient Noise Levels*

Sound pressure levels were greater during flood tide than at slack water, as measured by both the hydrophone on the bottom pod and on the drifter. The noise below 2 kHz is thought to originate from boat traffic (specifically propeller cavitation and engine noise), and to a lesser extent from the surface noise of waves breaking on the shoreline [18]. The high noise levels in the low frequency band (0-2 kHz) during the ambient noise drifts were due to windy conditions.

The ambient noise drifter (Fig. 9) should be less subject to pseudosound than the stationary bottom pod since efforts were taken to decouple the hydrophone from the flow. It was therefore expected that ambient noise level as a function of flow speed would be greater for bottom pod deployments than for the drifter. The drifter might not have been completely decoupled from the surface movement of the buoy, in which case the drifter would have been subject to pseudosound. A varying depth of the drifting hydrophone could lead to pressure fluctuations and contaminate data [19], especially at low frequencies (<1 kHz) [11]. Alternatively, the lower ambient noise levels registered by the hydrophones on the bottom pod could be due to the lower current speeds near the seabed and their associated low-pressure fluctuations caused by water moving around the hydrophone [14].

Since pseudosound is expected to be much lower at high frequencies, the peak noise levels at high frequencies – *i.e.* above 20 kHz – registered by both the drifting and stationary hydrophones are likely real. Bedload transport from tidal currents could explain the increased ambient noise levels that were observed in all frequency bands during peak flood (Figs. 7, 9), especially across the higher frequency bands. It has previously been shown that acoustic energy arises from inter-particle collisions of coarse sediment, and that greater sound pressure levels exist in higher frequencies for smaller particles [20]. Additionally, observed high intensity sounds (120-140 dB re 1 µPa) concurrent with the tidal signal have been attributed to the fast flow speeds that mobilize gravel and shell hash on the seabed [11, 12]. Shortly after these experiments (in Sept 2012), sediment samples were taken near the bottom pod site. This region revealed gravel to sand, with shell hash and a fine sediment top layer [17]. High-frequency (1 kHz to 200 kHz) sediment-generated noise can trigger detections of marine mammal echolocation clicks on automated detectors, and this has implications for passive acoustic monitoring [12, 21].

The results presented here indicate that there is considerable spatial variability in the ambient noise levels in Grand Passage. Background noise levels have been found to be higher in areas experiencing greater tidal current speeds than in more sheltered areas [9]. For any future PAM system at this site, this variability should be taken into account when choosing hydrophone locations (*i.e.* choose areas with weaker tidal currents). Tidal current models and ADCP measurements revealed areas of increased flow speeds (Fig. 1), and these are likely indicative of noisier areas, as was the case for the bottom pod location in the northwest of Grand Passage.

B. *Pseudosound Reduction*

The only noise reduction technique that appeared to greatly reduce background noise levels was the "sock" (Fig. 8). However, noise level reductions were least pronounced in the low frequency band in which pseudosound was anticipated (Table 2). The reduction of noise was prominent in the mid-low frequency band, but this overlapped with frequency of sound projections. This reduction of noise level is comparable to what was observed previously [13], as their 3 cm thick open cell foam flow shield reduced noise by up to 24 dB below 50 Hz.

While this field experiment started during the peak spring tide, the tide was weaker each succeeding day. This must be considered when comparing ambient noise levels of different bottom pod set-ups. Direct comparisons between pseudosound reduction techniques can be made when considering flow noise versus current speed (Fig. 8).

C. *Acoustic Detection Ranges*

Acoustic detection ranges were greatest for the bare vertical hydrophones. While a horizontal orientation positions the hydrophone closer to the seabed where current speeds are lower, a vertical hydrophone was deemed to be more appropriate for PAM since its sound measurements are less directional.

While ambient noise levels were lower across all frequency bands for the "sock" hydrophone (Table 2), its acoustic detection range is less than for the bare vertical hydrophone. The acoustic detection range of the "sock" was expected to be greatest because of the significant reduction of noise level in the frequency band in which the *ic*Talk was projecting sounds (2-20 kHz). It is therefore surprising that the highest maximum values of ΔCorr at close range are not seen in the "sock" hydrophone set-up. Instead, it is likely that the "sock"

attenuated the projected chirps from the *ic*Talk in addition to reducing pseudosound. This is evidenced by the reduction of noise levels in all frequency bands for the "sock", including the high frequency bands not associated with pseudosound (Table 2). Therefore, this pseudosound reduction technique is not recommended.

A previous experiment found that a flow shield significantly suppressed much of the noise increase from pseudosound at low frequencies (<750 Hz), when compared with an unshielded hydrophone, at flow speeds up to 1 m/s [11]. Their hydrophones, with and without flow shields, recorded equivalent levels of sound >750 Hz, and suggested that their flow shield effectively reduced pseudosound without attenuating propagating sound [11]. It appears that the same cannot be said for this experiment, where the "sock" is the flow shield.

The false alarm rate of detected chirps increased with increasing distance from the hydrophone, due to sound attenuation over distance (Fig. 8). While it makes sense for the maximum values of ΔCorr to decrease with distance from the hydrophone frame, it is less obvious why the observed values spike upwards at great distances (Fig. 8). The range at which false alarm rate was 50% was greatest for the bare vertical hydrophone, at ~700 m (Fig. 12).

The projected frequency range (2-20 kHz) was limited by the *ic*Talk, and was not fully representative of the range of local marine mammal vocalisations. Since marine mammals produce a variety of sound in different frequency ranges, the *ic*Talk would have ideally projected sounds as low as 20 Hz to mimic fin whale calls, and up to 130 kHz to imitate harbour porpoise clicks [3].

Sound transmission in shallow waters is highly variable due to the influence of acoustic properties of the seabed, surface, and the channel geometry/bathymetry [18]. The present research could be extended to include propagation models, and compare predicted to observed acoustic detection ranges.

V. Conclusion

The aim of this study was to obtain baseline ambient noise levels and sound detection ranges as a partial basis for determining the feasibility of a PAM system for marine mammals in Grand Passage, NS, prior to in-stream tidal energy development. The measurements reported here, made in July 2012, included both ambient noise measurements and a sound projection experiment to determine acoustic detection range, both as a function of tidal current speed. For the analysis of the projection experiment data, chirp correlator and peak detector functions were constructed in Matlab. Pseudosound reduction techniques were field tested, and a freely drifting hydrophone characterised ambient noise levels.

Sound pressure levels at peak flood were ~25 dB greater than during slack water. Efforts to reduce pseudosound were not very successful. The "sock" set-up resulted in the greatest noise suppression, but also the worst detection ranges, whereby it reduced sound pressure levels in frequency ranges extending beyond those affected by pseudosound (<1 kHz), suggesting that the projected chirps were attenuated by open-cell foam. Acoustic detection ranges were greatest when the hydrophone was bare and vertical, and extend up to ~700 m from the bottom pod location in the northwest of Grand Passage. Ambient noise levels were modulated by both water speed and location within the channel. Peak noise levels at high frequencies – 10 kHz and higher – during high flow are attributed to collisions among the mobile sediments on the seabed, predominantly shell hash in Grand Passage.

The present work contributes to the future acoustic monitoring of marine mammal presence in the vicinity of the proposed tidal turbine. This information will help inform future monitoring of marine mammal sounds near in-stream tidal turbine sites, laying a basis for site-specific marine mammal event detections. Acoustic propagation modelling of Grand Passage would also be useful. Future investigations should include longer acoustic recording deployments, measurements in different seasons, projections over a wider frequency range, and an investigation into how acoustic detection ranges change as a function of projected frequency; these would increase the understanding of shallow water acoustics in Grand Passage.

Acknowledgment

This study was funded by a Natural Sciences and Engineering Research Council (NSERC) ENGAGE grant to the Ocean Acoustics Lab at Dalhousie University and Ocean Sonics (Great Village, NS), and by a Nova Scotia Strategic Co-operative Education Incentive grant for undergraduate Science Co-op students. This work was also carried out in collaboration with Greg Trowse of Fundy Tidal Inc. Thanks are extended to Justine McMillan, Matthew Hatcher, and Nina Stark, as well as the captain and crew of the *Expectations XL*, for their assistance in the field, and to Mark Wood, Jay Abel, Walter Judge and Doug Schillinger for technical support.

References

[1] R. Inger, M. J. Attrill, S. Bearhop, A. C. Broderick, W. J. Grecian. D. J. Hodgson, and B. J. Godley. "Marine renewable energy: potential benefits to biodiversity? An urgent call for research," *Journal of Applied Ecology*, vol. 46, pp. 1145-1153, Dec. 2009.

[2] L. D. Murison, and D. E. Gaskin. "The distribution of right whales and zooplankton in the Bay of Fundy, Canada," *Canadian Journal of Zoology*, vol. 67, pp. 1411-1420, Jun. 1989.

[3] C. E. Malinka, "Acoustic detection ranges and baseline ambient noise measurements for a marine mammal monitoring system at a proposed in-stream tidal turbine site: Grand Passage, Nova Scotia," B. Sc. Thesis, Dalhousie University, Halifax, Canada, May 2013.

[4] C. E. Malinka, M. W. Brown, G. T. Trowse, B. Winney, and V. Zetterlind. "Observations of marine mammals in Petit Passage and Grand Passage, Nova Scotia and adjacent waters in the eastern Bay of Fundy to assess species composition, distribution, number and seasonality," Tech. Rep. for the Nova Scotia Offshore Energy Research Association (OERA), 44 p., Jan 2015.

[5] S. Dolman and M. Simmonds. "Towards best environmental practice for cetacean conservation in developing Scotland's marine renewable energy," *Marine Policy*, vol. 34, issue 5, pp. 1021-1027, Sept. 2010.

[6] H. A. Viehman, "Fish in a tidally dynamic region in Maine: Hydro acoustic assessments in relation to tidal power development," M. Sc. Thesis, University of Maine, U.S.A., May 2012.

[7] B. Wilson, R. S. Batty, F. Daunt, and C. Carter. "Collision risks between marine renewable energy devices and mammals, fish and diving birds," Scottish Association for Marine Science, Oban, Scotland, Tech. Rep. PA371QA, 2009.

[8] D. J. Tollit, J. D. Wood, J. Broome, and A. M. Redden. “Detection of marine mammals and effects monitoring at the NSPI (OpenHydro) turbine site in the Minas Passage during 2010,” Fundy Ocean Research Centre for Energy, Nova Scotia, Canada, Tech. Rep., 2011.

[9] M. Willis, M. Broudic, C. Haywood, I. Masters, and S. Thomas. “Measuring underwater background noise in high tidal flow environments,” *Renewable Energy*, vol. 49, pp. 55-58, Jan. 2013.

[10] C. Bassett, J. Thomson, and B. Polagye. “Characteristics of underwater ambient noise at a proposed tidal energy site in Puget Sound,” in *OCEANS 2010 IEEE*, 2010, p. 1-8.

[11] B. Polagye, J. Thomson, C. Bassett, J. Graber, R. Cavagnaro, J. Talbert, A. Reay-Ellers, D. Tollit, J. Wood, A. Copping, *et al*. “Study of the acoustic effects of hydrokinetic tidal turbines in Admiralty Inlet, Puget Sound,” U. S. Department of Energy, Tech. Rep., 2012.

[12] C. Bassett, J. Thomson, and B. Polagye. "Sediment-generated noise and bed stress in a tidal channel." *Journal of Geophysical Research: Oceans*, vol. 118(4), pp. 2249-2265, Apr 2013.

[13] S. Lee, S.-R. Kim, Y. K. Lee, J. R. Yoon, and P.-H. Lee. “Experiment on effect of screening hydrophone for reduction of flow-induced ambient noise in ocean,” *Japanese Journal of Applied Physics*, vol. 50, Jul. 2011.

[14] B. Martin, C. Whitt, C. McPherson, A. Gerber, and M. Scotney. “Measurement of long-term ambient noise and tidal turbine levels in the Bay of Fundy,” in *Proc. AAS'12,* 2012, p.1-7.

[15] G. Trowse, and R. Karsten. “Bay of Fundy tidal energy development – opportunities and challenges,” in Proc. of International Conference on Ocean Energy (ICOE), p. 1-11, Bilbao, Spain, Oct 2010.

[16] J. M. McMillan, A. E. Hay, R. H. Karsten, G. Trowse, D. Schillinger, and M. O’Flaherty-Sproul., “Comprehensive Tidal Energy Resource Assessment in the lower Bay of Fundy, Canada,” in Proc. of European Wave and Tidal Energy Conference (EWTEC), p. 1-10, Aalborg, Denmark, 2013.

[17] N. Stark, A. E. Hay, and G. Trowse. “Cost-effective geotechnical and sedimentological early site assessment for ocean renewable energies,” in Proc. Of European Wave and Tidal Energy Conference (EWTEC), p. 1-8, Aalborg, Denmark, 2013.

[18] W. J. Richardson, C. R. Greene, S. I. Malme and D. H. Thomson. *Marine Mammals and Noise*. USA: Academic Press, 1995.

[19] P. Stein. (2011) Radiated noise measurements in a high current environment using a drifting noise measurement buoy (part B). In DOE Marine Hydrokinetics Webinar 3: Monitoring technologies and strategies. U.S. Department of Energy. Available: http://mhk.pnnl.gov/publications/doe-mhk-webinar-3-monitoring-technologies-and-strategies.

[20] P. D. Thorne. “Laboratory and marine measurements on the acoustic detection of sediment transport,” Journal of the Acoustical Society of America, vol. 80, pp. 899-910, 1986.

[21] C. E. Malinka, J. D. J. Macaulay, J. Gordon, and S. Northridge. “Evaluation of a drifting porpoise localizing array buoy: a novel configuration for tracking porpoises in tidal rapids using passive acoustics,” Internship report under the Marine Renewable Energy Knowledge Exchange Programme, March 2015, p. 1-24.